

Optimization-based Tuning of Low-bandwidth Control in Spatially Distributed Systems

Dimitry Gorinevsky*, Stephen Boyd† and Gunter Stein‡

September 2002

Abstract

We describe a new method for tuning a certain family of low-bandwidth controllers for linear time-invariant and spatially-invariant (LTSI) plants. We consider LTSI controllers with a fixed structure, which is PID in time and local in spatial coordinates. Two spatial feedback filters, assumed to be symmetric and have finite spatial response, modify the local PID control signal based on the error and control signals, respectively, at nearby nodes. Like an ordinary PID controller, this controller structure is simple, but provides adequate performance in many practical settings.

We cast a variety of specifications on the steady-state spatial response of the controller as a set of linear inequalities on the design variables, and so can carry out the design of the spatial filters using linear programming. The method handles steady-state limits on actuator signals, error signals, and several constraints related to robustness to plant and controller variation. While the method does *not* directly handle some important constraints involving the effects of boundary conditions, or guaranteed closed-loop spatial or time decay, it does appear to work very well for low-bandwidth controllers, and so is applicable in a variety of practical situations.

*Honeywell AES Guidance, Navigation, and Control Laboratory, 1 Results Way, Cupertino, CA 95014; email: gorinevsky@ieee.org; dimitry.gorinevsky@honeywell.com; phone: (408) 864-7569, e-fax: (208)545-6408

†Information Systems Laboratory, Electrical Engineering Department, Stanford University; email boyd@stanford.edu

‡Honeywell

1 Introduction

Proliferation of embedded computing, and the maturing of actuator and sensor technologies has led to growing importance of spatially distributed system control technology. In such systems spatial profiles (distributions) of physical variables are controlled using arrays of actuators and sensors distributed over a spatial domain. Array signal processing has had numerous practical applications for quite some time; array control technology is presently emerging.

Much of the expected growth in array control technology area is related to development of Micro-Electro Mechanical Systems (MEMS), which allows low-cost production of large arrays of actuators and sensors. The computing might be distributed and embedded with the actuators.

Apart from such potential future applications, array control systems can be encountered in multiple types of industrial processes, and have been used in some cases for a long time. For example, a core of a nuclear reactor usually contains a 2-D array of control rods used to regulate temperature and neutron flux in the active zone. Perhaps the most widespread industrial application is control of flat sheet processes, such as paper manufacturing, where linear arrays of up to 300 actuators might be employed. There are also diverse array control applications related to thermal processing, including Rapid Thermal Processing in semiconductor manufacturing, crystal growth control, and material heating processing. In all of these applications, spatial profiles of temperature are controlled using arrays of heating elements.

Some more futuristic applications are being developed in the aerospace area. Flow control using large arrays of microactuators distributed over on an airfoil or a channel boundary is one of them. Another area is ‘smart structure’ control of lightweight space reflector shape. (A 1-D distributed reflector control problem is considered in this paper as an example.) This is closely related to adaptive optics, where large 2-D arrays of actuators are used to deform a reflecting surface to achieve wavefront control.

Various mathematical approaches to analysis and design of feedback control in large (or infinite) distributed systems with regular array structure were proposed and explored in a number of publications. The most relevant to this paper are [1, 2, 4, 5, 7], where further references can be found. Most of this work is focused on design of high-performance spatially invariant feedback control systems, with performance and robustness guarantees. Our goals are less ambitious; we focus on tuning methods for distributed generalizations of low bandwidth PID controllers.

In this paper, we consider a spatially distributed system analog of low-bandwidth PID control. A standard PID controller uses three values of the plant output (current, past and the integral) for computing the control. In a similar way the ‘spatial PID’ controller considered in this paper uses data from a few neighboring array cells. Such an approach is justified by its computational simplicity. This is important for centralized implementation of the array con-

trol because of the potential issues with the computing power needed for control of hundreds or thousands of actuators. Such control algorithms can be also conveniently implemented as decentralized computations in an array with distributed embedded computing. In the latter case, parallel processing makes computing performance less of an issue but constraints on communication between the processors become important; local communication with the nearest neighbors can be performed most efficiently. The spatial PID controller architecture considered in this paper, like an ordinary low-bandwidth PID controller, provides adequate performance in many, or even most, practical situations. Also like an ordinary low-bandwidth PID controller, it is not meant to provide performance at or near the limit of possible performance; it is meant to be a simple control architecture that provides adequate performance, after proper tuning, in a large number of practical cases.

An approach closely related to ours is spatial loopshaping design (or tuning) of a distributed controller, as discussed in [10, 11]. Spatial loopshaping allows accommodating many important engineering specifications for controller design. The localized controller in [10, 11] is obtained by designing of a non-localized controller, which is then truncated to provide a localized controller.

The contribution of this paper is the formulation of the spatially distributed controller design (tuning) problem as a convex optimization problem. Localized spatial (FIR) operators are assumed at the outset, and the main engineering specifications are accommodated within a linear programming (LP) optimization framework. This allows for a computationally efficient and conceptually clean one-shot solution for the optimal FIR weights in the controller.

We will see that the conversion of the problem to an LP is possible because the spatial responses considered are *symmetric*. This makes the spatial transfer functions (numerator and denominator) *real* and enables us to convert linear fractional (closed-loop) design constraints into linear constraints. The same trick does not work in the absence of symmetry.

The idea that symmetry of a pulse response leads to a real transfer function, and therefore limits on the frequency response can be expressed as linear inequalities, is not new; it is the basis of linear programming based design of symmetric FIR filters for signal processing applications, which has been done at least since 1969 (see [3, p.380]). In this paper, however, we consider closed-loop expressions, which are *linear fractional* expressions in the FIR filter weights. As far as we know, this has not been done before.

2 Plant model

In this paper an array control system will be modeled as a linear time-invariant spatially-invariant (LTSI) system. This model does not consider boundary effects present in a finite array (unless it has a circulant structure). An LTSI model allows for an efficient multidimensional

frequency-domain analysis of the problem. Note that an analysis involving spatial frequencies can be considered as modal analysis of the system dynamics, since the spatial sinusoids are the eigenmodes of a spatially invariant system [1]. Boundary condition issues (which arise when the true plant and controller are not spatially infinite) are outside of the paper scope, but they can be (at least partially) integrated into the framework described here. This is a subject of ongoing research.

Consider a two-dimensional (2-D) distributed system evolving in the integer time $t = 0, 1, \dots$ and with an integer spatial coordinate $x = \dots, -1, 0, 1, \dots$ indexing the actuator cells. (We assume that x ranges over all integers; in reality, the number of actuators is always finite. In what follows, we ignore the issue of (finite) boundaries, except in the simulation example.) The (scalar) actuator or control signal will be denoted $u = u(t, x)$, which is the control applied by actuator number x in the array, at time t . The (scalar) process output is $y = y(t, x)$, where one measurement per actuator, and per time sample, is assumed. A general input-output model of an LTSI plant has the 2-D convolution form

$$y(t, x) = \sum_{k=0}^{\infty} \sum_{n=-\infty}^{\infty} h(t - k, x - n)u(k, n), \quad (1)$$

where $h(t, x)$ is the system 2-D pulse response function, or system Green's function.

We will assume a *separable* plant model, which has the form

$$h(t, x) = h_t(t)h_x(x), \quad (2)$$

where $h_t(t)$ is the plant time pulse response, and $h_x(x)$ is the plant spatial pulse response. We assume that h_t is causal, i.e., $h_t(t) = 0$ for $t < 0$. We will also assume that the plant is spatially symmetric, which means that $h_x(-x) = h_x(x)$. (The same methods work for plants that are spatially anti-symmetric, i.e., satisfy $h_x(-x) = -h_x(x)$.)

Such a model is applicable in many distributed systems where actuator dynamics or sensor dynamics or dynamics of a fixed dynamical filter are dominant. These dominant time dynamics are described by the time response $h_t(t)$ while $h_x(x)$ gives the steady-state spatial response shape. Separable models of the form (2) are used in many practical applications of array control including web processes and adaptive optics. Note that the separable model (2) can be considered as a first dyadic term in a principal component analysis approximation of a general pulse response.

The analysis to follow uses a 2-D transfer function of the plant obtained by computing a z -transform of the pulse response (2). This transfer function has the form

$$H(z, \lambda) = g(z^{-1})G(\lambda) \quad (3)$$

where $g(z^{-1})$ is the z -transform of the causal dynamical pulse response $h_t(t)$ in (2) and $G(\lambda)$ is a spatial transfer function computed as the (two-sided) z -transform of the spatial pulse response (Green function) $h_x(x)$.

The plant is assumed stable and the spatial response absolutely summable (spatially stable). This means $g(z^{-1})$ is analytic inside the unit circle $|z| \leq 1$ in the complex plane, and $G(\lambda)$ is analytic inside an annulus of the form $r \leq |\lambda| \leq r^{-1}$, where $0 < r \leq 1$.

The plant model to be used in the control design and analysis is

$$y = g(z^{-1})G(\lambda)u \tag{4}$$

In this model z^{-1} can be interpreted as a unit time delay operator and λ as a unit positive spatial displacement operator. We assume that g and G are scaled so $g(1) = 1$, i.e., the time pulse function g is normalized to have unit static gain. Our assumption of spatial symmetry implies that the spatial transfer function G is *real* for $|\lambda| = 1$. (If the plant were spatially anti-symmetric, then G would be pure imaginary for $|\lambda| = 1$.)

3 Controller structure

As described in the introduction, we are interested in low-bandwidth control of the plant (4). The goal is to cancel the steady-state error in reaching the desired spatial profile $y_d(x)$. This goal can be achieved by using a controller structure given by

$$u = z^{-1}u - z^{-1}c(z^{-1})K(\lambda)(y - y_d) - z^{-1}S(\lambda)u \tag{5}$$

The first term in (5) introduces integration into the actuator signal path; the transfer function c in the second term corresponds to the particular controller used. The spatial filters K and S , which appear in the second and third terms, are used to improve the spatial response of the closed-loop system. They can be interpreted as regularization terms, which avoid inverting the plant at spatial frequencies where the plant gain is small [12]. Controllers of the form (5) have been used in web manufacturing processes [9, 6, 11].

We assume that the spatial filters $K(\lambda)$ and $S(\lambda)$ are FIR operators, which implies that the controller (5) is spatially localized; the control signal $u(t, x)$ is computed based on only a finite number of error and actuator signals, at nearby actuator cells. This reflects important communication and computing constraints. For a centralized controller (finite but large array) FIR operators K and S can be implemented with high computational efficiency as convolution kernels applied to the respective spatial variable profile; for a controller implemented through distributed embedded computing, K and S being FIR enables communication among a few near neighbors only.

The dynamical controller $c(z^{-1})$ in (5) (together with the integrator term) is a simple low-bandwidth controller, such as a PI or PID controller (considered in the example section), or a Dahlin controller (discrete-time Smith predictor), which is used in paper web manufacturing control. We can interpret the controller (5) as a simple LTSI generalization of the classical PID controller.

We will assume that the controller, like the plant, is spatially symmetric, i.e., K and S are symmetric FIR filters; $K(\lambda)$ and $S(\lambda)$ are real for $|\lambda| = 1$. (When the plant is spatially anti-symmetric, we assume that K is anti-symmetric, and S is symmetric.)

4 Closed-loop dynamics

We now consider the closed-loop dynamics for the system (4)-(5). As discussed in more detail in [1], an LTSI system can be diagonalized by the spatial sinusoids. By substituting $\lambda = e^{i\nu}$ we obtain the modal dynamics for the spatial frequency ν . With some overload of notation, the error dynamics for the mode at frequency ν are

$$e(t+1, \nu) = (1 - s(\nu))e(t, \nu) - l(\nu)g(z^{-1})c(z^{-1})e(t, \nu) + s(\nu)y_d(\nu), \quad (6)$$

where

$$y_d(\nu) = (2\pi)^{-1} \sum_x y_d(x) e^{i\nu x},$$

and $e(t, \nu) = y(t, e^{i\nu}) - y_d(\nu)$, and the modal loop gains are

$$l(\nu) = G(e^{i\nu})K(e^{i\nu}), \quad s(\nu) = S(e^{i\nu}) \quad (7)$$

Our assumptions of spatial symmetry of the plant and controller imply that GK and S are real for $|\lambda| = 1$, so the modal loop gain $l(\nu)$ and the modal smoothing gain $s(\nu)$ in (6) are real numbers. The equation (6) gives us another interpretation of our basic controller structure: it can be considered an independent PID (or other simple structure) controller, for each spatial frequency, or a family of PID controllers, one for each spatial frequency. The modal loop gain $l(\nu)$ and the modal smoothing gain $s(\nu)$ are determined by the coefficients of the spatial FIR filters K and S . Thus, the tuning of these filters can be interpreted as the problem of tuning a *family* of PID controllers, indexed by the spatial frequency ν .

Assume first that $s(\nu) = 0$. The modal error e will converge to zero provided that the loop gain $l > 0$ is sufficiently small and the steady-state gain of dynamical controller is such that $g(1)c(1) > 0$. The steady-state error in e is eliminated because of the integrator (a pole at $z=1$) present in the controller (5) for $S = 0$. The modal convergence can be made faster by increasing the loop gain l within certain limits $l(\nu) \leq L_0$. The specific value of L_0 and the details of tuning the integrator gain, depend on the plant transfer function $g(z^{-1})$ and controller transfer function

$c(z^{-1})$ and will not be discussed here. The only design specification we will use for achieving low-bandwidth modal control is the one already mentioned,

$$0 < l(\nu) \leq L_0, \quad (8)$$

which limits the loop gain to be less than a given limit L_0 , at all spatial frequencies.

We can interpret the smoothing operator S as a regularizing term that handles the case when the plant spatial gain is very small, or zero. To see this, suppose the plant gain $G(e^{i\nu})$ is zero or very small at some spatial frequency ν . In accordance with (4), for this mode the plant output $y(t, \nu)$ can be assumed to be zero. Hence the dynamics (5) of the control input at this spatial frequency can be approximated as

$$u(t+1, \nu) = (1 - s(\nu))u(t, \nu) + c(z^{-1})K(e^{i\nu})y_d(\nu). \quad (9)$$

Here the term $s(\nu)$, provided it is positive, can be interpreted as introducing some leakage into the integrator in the controller. Without any smoothing, i.e., with $s(\nu) = 0$, however small the controller gain $K(e^{i\nu})$ is, the integrator in (5) will keep integrating until the actuator signal becomes extremely large. The operator S (and the gain $s(\nu)$ has an effect of regularizing the ill-defined problem of controlling a distributed plant with some zero modal gains. It is often called a ‘smoothing’ operator because small gain is usually associated with high spatial frequencies and the regularization has an effect of reducing the large amplitude of high frequency components in the control signal u .

5 Specifications for controller tuning

The goal of this paper is to formulate an optimization approach to tuning the spatial FIR operators K and S in the controller (5). The main emphasis is on low-bandwidth control; we take the maximum loop gain condition (8) as the only condition related to the time-domain loop dynamics. As touched upon in the previous section, the main issues with low-bandwidth control are related to steady-state closed-loop response, i.e., the response for $z = 1$. By combining (4) and (5) the closed-loop spatial transfer functions can be obtained. The error $e = y - y_d$ and control u in steady-state (i.e., at $z = 1$), and at spatial frequency ν ($\lambda = e^{i\nu}$), are given by

$$e = \frac{S(e^{i\nu})}{S(e^{i\nu}) + G(e^{i\nu})k_I K(e^{i\nu})} y_d(\nu), \quad (10)$$

$$u = \frac{k_I K(e^{i\nu})}{S(e^{i\nu}) + G(e^{i\nu})k_I K(e^{i\nu})} y_d(\nu), \quad (11)$$

where the integrator gain is $k_I = c(z = 1)$. Recall that $g(z = 1) = 1$ is assumed.

For deriving engineering specifications on the control it will be assumed that a bound on the target profile y_d is available in the form $|y_d(\nu)| \leq d_0$, i.e., we have a known bound on the

maximum of the of the target profile at every frequency. We require that for any such target profile, the magnitude of the control is bounded for all spatial frequencies, i.e., $|u| \leq u_0$) for all ν . Using (11), the last condition can be expressed in the form

$$\left| \frac{k_I K(e^{i\nu})}{S(e^{i\nu}) + G(e^{i\nu})k_I K(e^{i\nu})} \right| \leq u_0/d_0, \quad \text{for all } \nu. \quad (12)$$

In a similar way we require that the magnitude of the steady-state error is bounded, i.e., $|e| \leq e_0$ for all ν in the band of spatial frequencies $B \subseteq [0, \pi]$ over which we require good control performance. This leads to the steady-state performance condition

$$\left| \frac{S(e^{i\nu})}{S(e^{i\nu}) + G(e^{i\nu})k_I K(e^{i\nu})} \right| \leq e_0/d_0, \quad \text{for all } \nu \in B. \quad (13)$$

Unlike (12), which is required to hold for any spatial frequency ν , the small steady-state error condition (13) is required only within the spatial bandwidth of the system, $\nu \in B$. This bandwidth might be taken, for example, as the set of the spatial frequencies where the plant gain is sufficiently large to ensure that the disturbances can be compensated without an excessive control effort, i.e.,

$$\left\{ \nu \in B : |K(e^{i\nu})| \geq k_0 \right\}.$$

Another important engineering requirement is the robustness of the closed-loop system to plant modeling error. Assume that instead of the plant description (4), we have the following perturbed plant,

$$y = g(z^{-1})G(\lambda)u + \delta P(z^{-1}, \lambda)u, \quad (14)$$

where $|\delta P| \leq \delta_0$ for $|z| \leq 1$, $|\lambda| = 1$. The small gain theorem guarantees stability of the closed-loop system with perturbed plant (14), and the controller (5), provided

$$\left| \frac{c(z^{-1})K(\lambda)}{1 - z^{-1} + z^{-1}S(\lambda) + z^{-1}c(z^{-1})g(z^{-1})G(\lambda)K(\lambda)} \right| \delta_0 < 1 \quad \text{for } |z| = 1, |\lambda| = 1. \quad (15)$$

Since in low-bandwidth control the main control action takes place at low dynamical frequencies, a steady-state robustness condition will be considered in place of (15). For $|z| = 1$, (15) reduces to

$$\left| \frac{k_I K(\lambda)}{S(\lambda) + k_I G(\lambda)K(\lambda)} \right| \delta_0 < 1 \quad \text{for } |\lambda| = 1. \quad (16)$$

We can also consider robustness to controller variations. A distributed controller implementation might differ from the designed controller, for several reasons: our analysis does not take boundary effects into account; and we may have sensor, actuator, or computing element faults in the distributed control system. Assume that instead of the nominal controller (5), we have

$$u = z^{-1}u - c(z^{-1})K(\lambda)(y - y_d) - z^{-1}S(\lambda)u + \delta C(z^{-1}, \lambda)u, \quad (17)$$

where $|\delta C| \leq \delta_C$ for $|z| \leq 1$, $|\lambda| = 1$. Similar to how (16) is derived, the small-gain based steady-state robustness condition can be expressed in the form

$$\left| \frac{S(\lambda)}{S(\lambda) + k_I G(\lambda) K(\lambda)} \right| \delta_C < 1 \quad \text{for } |\lambda| = 1. \quad (18)$$

Finally, we consider robustness to variations in the smoothing operator S . Assume that in (5) the smoothing operator is $S(\lambda) + \delta S(z^{-1}, \lambda)$, where $|\delta S(z^{-1}, \lambda)| \leq \delta_S$ for $|z| \leq 1$, $|\lambda| = 1$. Once again, we can derive a small-gain based robustness condition:

$$\left| \frac{1}{S(\lambda) + k_I G(\lambda) K(\lambda)} \right| \delta_S < 1 \quad \text{for } |\lambda| = 1. \quad (19)$$

In summary, the specifications are given by the loop-gain limit for dynamic stability (8), and

- the actuator limit (12)
- the performance specification (13)
- robustness to plant variation (16)
- robustness to controller variation (18)
- robustness to smoothing operator variation (19).

Since the loop gain $l(\nu)$ is a linear function of $K(\nu)$, the loop gain constraint consists of a lower bound (i.e., 0) and an upper bound (L_0) on a linear function of K , for each frequency ν . Each of the other specifications has the form of a limit on the magnitude of a linear fractional function of $K(\lambda)$ and $S(\lambda)$, for all $|\lambda| = 1$, or (in the case of the performance specification) for some $|\lambda| = 1$.

6 Optimization formulation

We now show how the design of the spatial filters K and S can be cast as a semi-infinite convex optimization problem, which can be approximated well as a linear program (and therefore solved efficiently). As briefly mentioned in Section 3, these operators are constrained to be FIR operators such that information from near neighbors only is used when computing control at a particular spatial location.

In the case when the FIR operator K is symmetric (which we assume when G is symmetric), we can express it as

$$K(\lambda) = \kappa_0 + \sum_{k=1}^N (\lambda^k + \lambda^{-k}) \kappa_k, \quad (20)$$

where $\kappa_0, \dots, \kappa_k$ are the coefficients. When $G(\lambda)$ is anti-symmetric, we take K to be anti-symmetric as well, in which case it has the form

$$K(\lambda) = \sum_{k=1}^N (\lambda^k - \lambda^{-k}) \kappa_k. \quad (21)$$

(We will explain the method assuming that K and G are symmetric.) The smoothing FIR operator $S(\lambda)$ is always assumed to be symmetric, and has the form

$$S(\lambda) = \sigma_0 + \sum_{k=1}^N (\lambda^k + \lambda^{-k})\sigma_k, \quad (22)$$

where $\sigma_0, \dots, \sigma_N$ are the coefficients. At the spatial frequency ν , i.e., $\lambda = e^{i\nu}$, we have

$$K = \kappa_0 + 2 \sum_{k=1}^N \kappa_k \cos(k\nu), \quad S = \sigma_0 + 2 \sum_{k=1}^N \sigma_k \cos(k\nu).$$

Let $x \in \mathbf{R}^{2N+2}$ be the vector of all the coefficients, i.e., our optimization variables:

$$x = [\kappa_0 \ \cdots \ \kappa_N \ \sigma_0 \ \cdots \ \sigma_N]^T. \quad (23)$$

For each spatial frequency ν , K and S are linear functions of x , and therefore so are the loop and smoothing gains, $l(\nu)$ and $s(\nu)$.

We will now show how all of the tuning specifications can be expressed as (infinite) sets of linear inequalities on the variable x . For each ν , the loop-gain limit for dynamic stability (8), $0 \leq l(\nu) \leq L_0$, is a pair of linear inequalities in x .

Expressing the other constraints (which involve linear fractional functions) as linear constraints is not as straightforward. For each spatial frequency ν , the requirements (12), (13), (16), (18), and (19) have the form

$$\left| \frac{a^T x + b}{s(\nu) + k_I l(\nu)} \right| \leq 1, \quad (24)$$

where $a \in \mathbf{R}^n$ and $b \in \mathbf{R}$ (and depend on the spatial frequency, and also which specification is being represented). The second term in the denominator, $k_I l(\nu)$, is nonnegative, and is positive except at spatial frequencies where the plant gain is zero. In fact, the whole denominator must be positive at all spatial frequencies; indeed, the whole point of the smoothing operator S is to ensure $s(\nu) > 0$ for spatial frequencies where $l(\nu)$ is small. We can argue this as follows. Suppose the denominator (which is real) changes sign, and therefore is zero at some spatial frequency ν . At that frequency, the robustness to smoothing operator variation constraint, (19), is certainly violated, since the numerator of the relevant transfer function is a nonzero constant, and the denominator vanishes, so the relevant transfer function is infinite (and certainly not less than one in magnitude). Thus, we have

$$s(\nu) + k_I l(\nu) > 0 \quad \text{for all } \nu, \quad (25)$$

for any controller that satisfies all the specifications. Since the denominator is positive, we can multiply through by it, and express the linear fractional constraint (24) as

$$-(s(\nu) + k_I l(\nu)) \leq a^T x + b \leq s(\nu) + k_I l(\nu). \quad (26)$$

This is a pair of linear inequalities in the variable x , since both $s(\nu)$ and $l(\nu)$ are linear functions of x .

Finally, we consider the objective. Roughly speaking, we want the (dynamic) loop gain as large as possible (to give us rapid convergence), while respecting the limit $l_0(\nu) \leq L_0$ for all ν . We can achieve this goal, approximately, by taking as objective

$$\phi(x) = \max_{\nu \in B} |l(\nu) - L_0/2|. \quad (27)$$

In other words, we try to have the loop gain approximate the target loop gain $L_0/2$ for the spatial frequencies in our control bandwidth. Since this objective is the maximum of a family of convex functions (absolute values of linear functions), it is a convex function of x . If ϕ is small, then we can expect approximately constant rate of convergence of the closed-loop system, over all spatial frequencies in B .

Thus, the overall design problem is a convex optimization problem:

$$\begin{aligned} & \text{minimize} && \phi(x) \\ & \text{subject to} && \text{linear inequalities (26) above, for each } \nu. \end{aligned}$$

The objective is given in (27), and the constraints are an infinite set of linear inequalities; specifically, ten per spatial frequency ν . (Such a problem is called *semi-infinite* since the constraints are indexed by the real number ν .)

Finally, we approximate the semi-infinite convex problem as an LP. We take a finite but sufficiently dense set of spatial frequencies, $\{\nu_1, \dots, \nu_M\}$, and impose all of the linear inequalities at these frequencies only. This results in a large, but finite, number of linear inequalities. Similarly, we approximate the objective by sampling over spatial frequencies:

$$\hat{\phi}(x) = \max_{\nu_i \in B} |l(\nu_i) - L_0/2|.$$

This is a piecewise linear and convex function of x . We can in turn formulate this sampled problem as a linear program, by introducing a new variable γ , and adding the constraints

$$-\gamma \leq l(\nu_i) - L_0/2 \leq \gamma, \quad \text{for } \nu_i \in B. \quad (28)$$

These constraints ensure that $\gamma \geq \hat{\phi}(x)$. Then we formulate the following linear program:

$$\begin{aligned} & \text{minimize} && \gamma \\ & \text{subject to} && -\gamma \leq l(\nu_i) - L_0/2 \leq \gamma, \quad \text{for } \nu_i \in B \\ & && \text{linear inequalities (26) above, for each } \nu_i. \end{aligned} \quad (29)$$

In this problem, the objective and all constraints are linear, i.e., it is a linear program (LP).

The LP (29) has $2N + 3$ variables ($2N + 2$ in case of anti-symmetric K), and no more than $12M$ linear inequality constraints. (The exact number depends on the number of spatial

frequency samples that fall in the control band B .) It can be solved very quickly for typical problem sizes, e.g., N several tens, and M several hundreds.

This method of synthesizing the spatial filters K and S can be used to tune the LTSI controller, by varying parameters in the specifications, such as the control band B , the actuator limit u_0 , the error limit e_0 , and the constants related to various types of uncertainty, i.e., δ_0 , δ_C , and δ_S . These parameters become the ‘knobs’ used by the control designer, that are varied to obtain adequate performance.

It should be clear from the discussion that many other specifications can also be included, and more complex specifications can also be handled by the method. As an example, we can impose a limit on loop gain that is a function of spatial frequency, instead of the constant L_0 used here. In addition, we can impose limits on the magnitude of *any* steady-state closed-loop spatial transfer function, since every one will be linear fractional, with the same denominator as the ones considered.

7 Simulation example

To illustrate our method for tuning an LTSI controller, we consider distributed control of a large-scale linear antenna reflector, describe in more detail in [8]. The plant model has the form (4), where

$$G(\lambda) = -\frac{\lambda - \lambda^{-1}}{\lambda - 2 - \theta + \lambda^{-1}}, \quad g(z^{-1}) = \frac{z^{-1}}{1 - az^{-1}}. \quad (30)$$

The anti-symmetric spatial response operator $G(\lambda)$ describes the pulse response of the reflector surface slope to the local actuator bending moment, as illustrated in Figure 1. The parameter a is a dynamical exponential factor describing the actuator response, and θ describes the relative effect of the beam tension and stiffness on the deformation in the Timoshenko beam model. A unit distance between the actuators is assumed. In the simulations, it was assumed that $a = 0.8$ (actuator time constant is 4-5 samples), and $\theta = 0.3$ (moderate tension in the beam). As a dynamical controller, a low-bandwidth PI controller was used, of the form (5), with

$$c(z^{-1}) = k_P(1 - z^{-1}) + k_I, \quad (31)$$

where the gains are $k_P = 0.3$ and $k_I = 0.1$.

Since the plant spatial operator $G(\lambda)$ in (30) is anti-symmetric, the operator K in the controller (5) is also chosen to be anti-symmetric, while S a symmetric operator. Both operators K and S have 3 FIR taps on each side off the center, i.e., $N = 3$. Since K is anti-symmetric, there are a total of seven coefficients in the FIR operators to be optimized.

The controller tuning problem was cast as an LP, as described above, with spatial frequency sampled at 128 points uniformly spaced in $[0, \pi]$. The controller specification parameters were chosen as follows:

- the loop gain limit is $L_0 = 0.4$ (so the target loop gain is $L_0/2 = 0.2$)
- the disturbance (target profile) bound is $d_0 = 0.1$
- the allowed control amplitude bound is $u_0 = 10 = 100d_0$
- the bandwidth B was taken as the set of spatial frequencies at which $|G(e^{i\nu})| \geq 0.2$
- the disturbance rejection (target profile tracking) error bound is $e_0 = 0.005 = 0.05d_0$
- the additive uncertainty in the integrator is $\delta_S = 0.00025L_0$

The solution to the described LP problem was found to be

$$\begin{aligned} [\kappa_1 \ \kappa_2 \ \kappa_3] &= [3.513 \quad -2.995 \quad 2.562], \\ [\sigma_0 \ \sigma_1 \ \sigma_2 \ \sigma_3] &= [0.344 \quad -0.268 \quad 0.213 \quad -0.105]. \end{aligned}$$

The engineering specifications (12), (13), and (28) for the designed controller are illustrated in Figure 2. The top plot illustrates the expected control amplitude—the lefthand side in (12)—computed as a function of the spatial frequency. The thin straight line is the righthand side constraint in (12). The middle plot in Figure 2 shows the expected error amplitude in the lefthand side of (13). The thin straight lines show the righthand side constraint. As one can see a low steady-state error is enforced within the plant bandwidth domain as shown by the extent of the constraint lines. The error grows rapidly outside of the bandwidth B . The loop gain $l(\nu)$ in the condition (28) is displayed in the bottom plot in Figure 2. The horizontal solid line in the middle corresponds to the target gain $L_0/2$. The robustness constraints (16)–(19) were less tight than the constraints (12), (13), (28) and therefore are not shown in Figure 2.

The designed controller was implemented in a simulation together with the described plant model. The simulation assumed a finite linear array of 100 actuator cells. The initial (jagged line) and final (much smaller) steady-state error obtained in the simulation are shown in the upper plot in Figure 3. Despite that fact that part of the disturbance (target) spectrum is uncontrollable, the achieved final error is very small compared to the initial error. The lower plot shows the steady-state actuator profile required to achieve this small final error. The initial actuator profile in the beginning of the simulation is zero.

In simulation, a very fast convergence to the steady-state is observed. The final steady-state error is achieved in 10-15 steps. The simulated time (and space) evolution of the closed-loop response to a single actuator pulse is illustrated in Figure 4. The lower plot shows the response of the output error, the upper plot shows the response of the control. One can see the fast convergence of the responses and the fact that high spatial frequencies close to the Nyquist frequency are not controllable.

References

- [1] Bamieh, B., Paganini, F., and Dahleh, M. “Distributed control of spatially-invariant systems,” *IEEE Trans. on Automatic. Contr.*, Vol. 47, No. 7, July 2002. pp. 1091 -1107.
- [2] Bose, N.K. *Applied Multidimensional Systems Theory*, Van Nostrand Reynhold, 1982
- [3] Boyd, S. and Barratt, C. *Linear Controller Design: Limits of Performance*, Prentice-Hall, 1991
- [4] D’Andrea, R. “Linear matrix inequality approach to decentralized control of distributed parameter systems,” *American Control Conf.*, Philadelphia, PA, pp.1350–1354, June 1998
- [5] D’Andrea, R., and Dullerud, G.E., “Distributed control of spatially interconnected systems,” *IEEE Trans. on Automatic Control* (to appear)
- [6] Duncan, S. R. , “The design of robust cross-directional control systems for paper making,” *American Control Conf.*, pp.1800-1805, Seattle , WA, 1995.
- [7] Gorinevsky, D., and Stein G., “Structured uncertainty analysis of robust stability for spatially distributed systems,” *IEEE Conference on Decision and Control*, pp. 3757 -3762, vol.4, Sydney, Australia, December 2000.
- [8] Gorinevsky, D., Hyde, T., and Cabuz, C. “Distributed shape control of lightweight space reflector structure,” *IEEE Conference on Decision and Control*, Vol. 4, pp.3850 -3855, Orlando, FL, December 2001,
- [9] Heaven,E.M., Jonsson, I.M.,Kean, T.M., Manness, M.A., and Vyse, R.N. “Recent advances in cross machine profile control,” *IEEE Control Syst. Mag.*, vol. 14, no. 5, Oct. 1994.
- [10] Stewart, G., Gorinevsky, D., and Dumont, G. “Design of a practical robust controller for a sampled distributed parameter system,” *37th IEEE Conf. on Decision and Control*, pp. 3156–3161, Tampa, FL, December 1998.
- [11] Stewart, G., Baker, P., Gorinevsky, D., and Dumont, G. “An experimental demonstration of recent results for spatially distributed control systems,” *American Control Conference*, pp. 2216 -2221, vol. 3, 2001, Arlington, VA, June 2001.
- [12] Tikhonov, A.N., and Arsenin, V.Ya. *Solutions of Ill-Posed Problems*. Halsted Press, Washington, 1977.

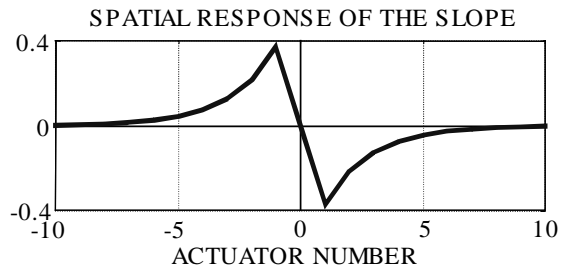


Figure 1: Spatial pulse response of the reflector surface slope

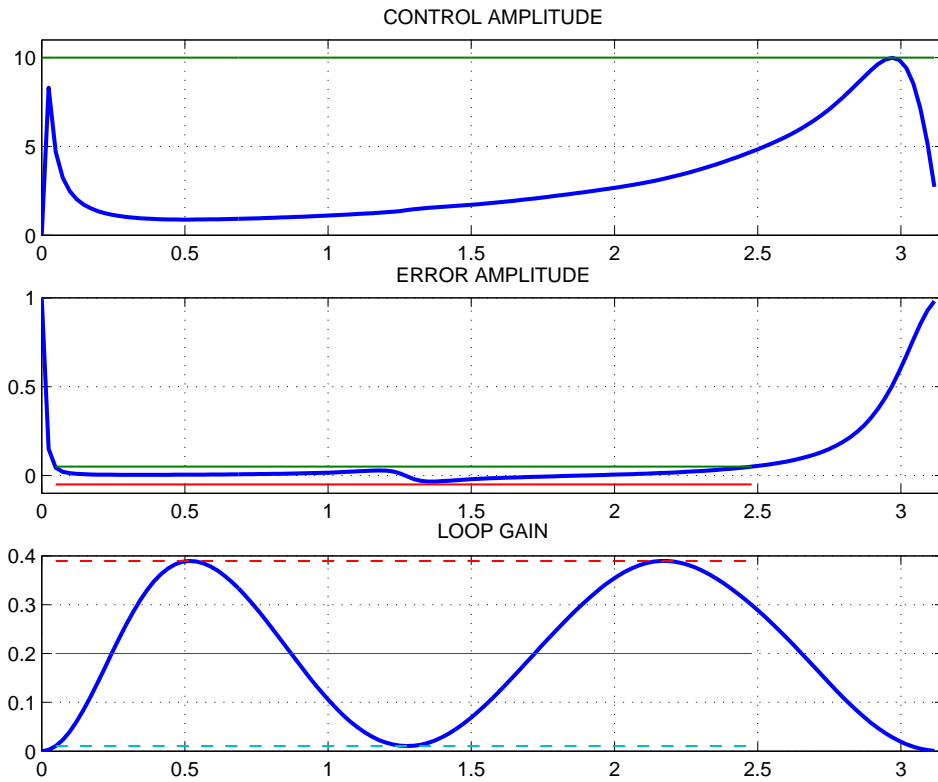


Figure 2: Steady-state loop shapes computed by the LP optimization

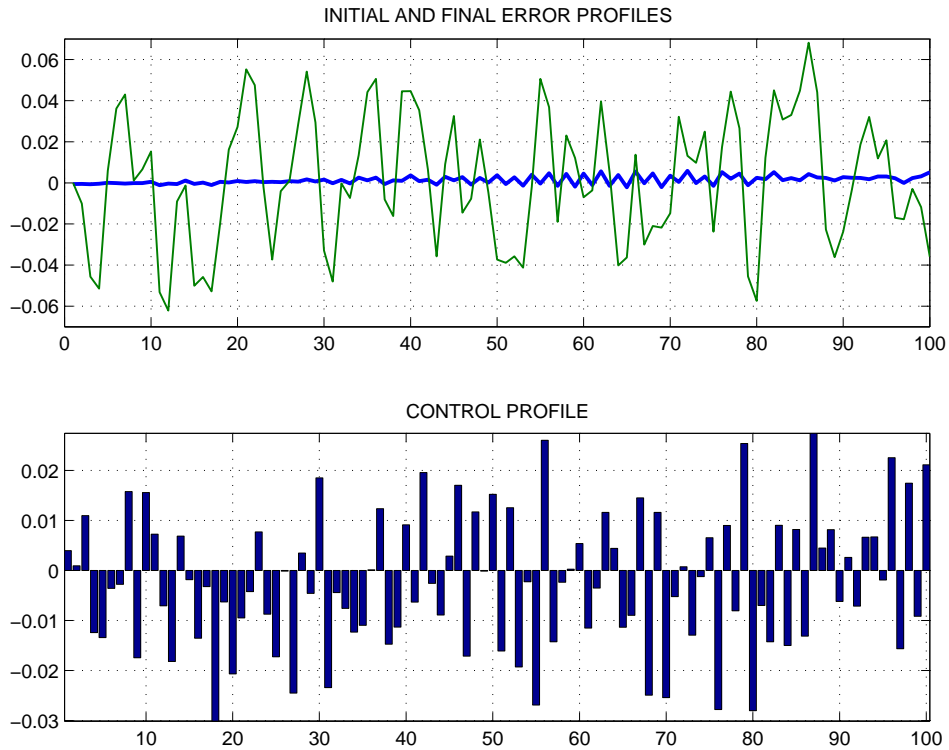


Figure 3: Steady-state disturbance compensation for a 'random' target profile

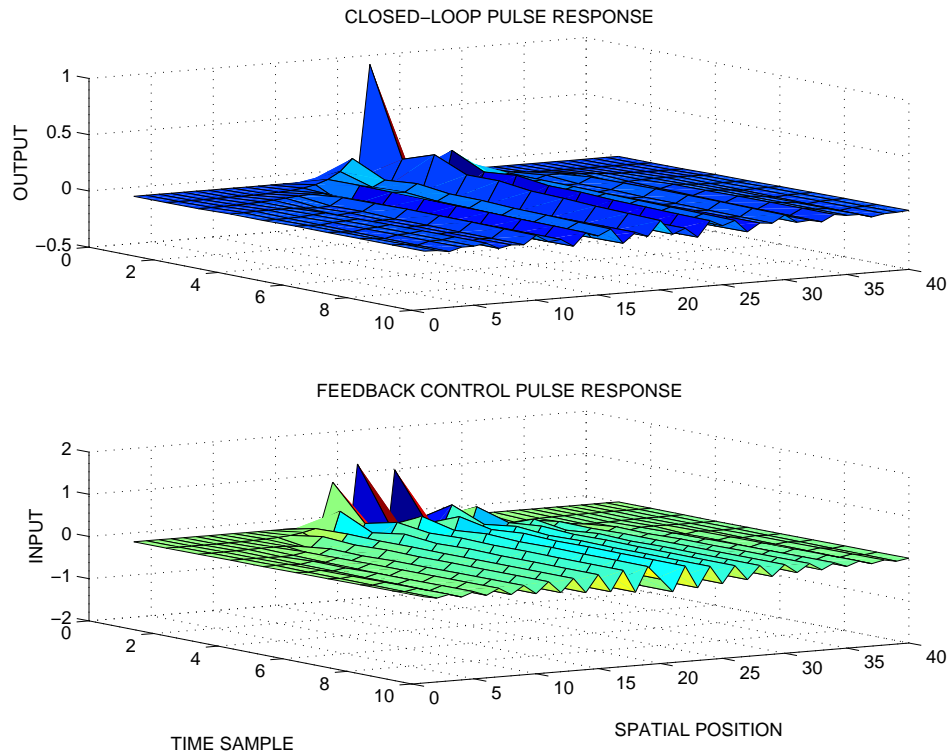


Figure 4: Steady-state disturbance compensation for a 'random' target profile